



Published in final edited form as:

Methods Mol Biol. 2019 ; 2009: 99–109. doi:10.1007/978-1-4939-9532-5_8.

Measuring *S*-depalmitoylation activity *in vitro* and in live cells with fluorescent probes

Rahul S. Kathayat, Bryan C. Dickinson

Department of Chemistry, The University of Chicago, GCIS E 319A, 929 E. 57th St., Chicago, IL 60637

Abstract

S-palmitoylation is a reversible lipid post-translational modification (PTM) that can mediate protein localization, trafficking, interaction with membranes, and a host of other biophysical characteristics. Over the past decade, a suite of chemoproteomic strategies have uncovered the breadth of *S*-palmitoylation, revealing widespread susceptibility to modification by this PTM throughout the human proteome. A focal point of research toward understanding the role of *S*-palmitoylation in varied cellular processes has focused on understanding how “writer” and “eraser” proteins function together to control the levels of *S*-palmitoylation of target proteins. The spatial and temporal regulation of *S*-palmitoylation by its “erasers” – acyl protein thioesterases (APTs) – is not fully understood. Tools which enable monitoring of the activity levels of the APTs in real-time in live cells illuminate how spatial control of these enzymes redecorate the lipidation state of the local proteome. To this end, we have developed fluorescence-based depalmitoylation probes (DPPs), which report *S*-depalmitoylase activity in live cells. Using DPPs, we have demonstrated that *S*-depalmitoylase activity alters in response to growth factor stimulation, unveiling potential regulation of cell growth and metabolism by APTs. Additionally, we recently discovered APTs in mitochondria using targeted DPPs, indicating new roles for dynamic *S*-palmitoylation in this metabolically critical cellular compartment. Here, we present detailed protocols on how to carry out *in vitro* *S*-depalmitoylase activity assays and live cell fluorescence imaging employing the growing DPP toolbox.

Keywords

Protein lipidation; *S*-Palmitoylation; acyl protein thioesterases; depalmitoylation; live-cell fluorescence imaging

1. Introduction

S-palmitoylation is an abundant lipid post-translational modification (PTM) that arises from the attachment of a C16 palmitate to the thiol of a cysteine residue through a thioester bond [1–3]. More than 10% of human proteome is reported to be susceptible to modification by *S*-palmitoylation [4], which makes it one of the most prevalent PTMs. Although thioesters are chemically stable in biological conditions, thioesters can be removed biochemically, making

palmitoylation one of the few dynamic lipid PTMs [5, 6]. Installation of the palmitate group (*S*-palmitoylation) is carried out in humans by 23 DHHC motif-containing palmitoyl acyl transferases (PATs), which are primarily associated with Golgi and ER membranes [2, 7–9]. Removal of the palmitate (*S*-depalmitoylation) is mediated by acyl protein thioesterases (APTs), which includes PPT1, APT1, APT2 and the ABHD17 family of proteins (A, B and C) [10–13]. PPT1 is a lysosomal protein, while APT1, APT2 and ABHD17A/B/C are generally thought to be cytosolic. However, we recently discovered that APT1 is also highly enriched in mitochondria [14].

The palmitoylation status of the proteome is not static, but instead can change in response to various input signals, such as growth factors [15, 16]. Measuring the palmitoylation status of the proteome can be achieved through a variety of proteomic methods such as acyl-biotin exchange (ABE) [17, 18], acyl-RAC [19], mass-shift assays [20], and metabolically labeling cells with clickable lipid analogues [21–23]. These techniques, however, report on changes to the palmitoylation level of target proteins, and do not reveal the mechanisms of those changes through alterations in the activities or localization of the PATs or APTs. Additionally, traditional proteomic methods don't generally reveal spatial information about how the activities of regulatory machinery result in local proteomic consequences. Indeed, we recently discovered both growth factor stimulation [24] and lipid stress [25] results in rapid alterations in the activities of the APTs. Therefore, probing the activities of the APTs, in real-time and in live cells, especially with spatial information, is critical to understanding the role(s) of the APTs in regulating cellular signaling.

The activities of the APTs can be monitored using activity-based protein profiling (ABPP) techniques employing general serine hydrolase probes [26] or APT-targeted probes [27]. Additionally, fluorescent substrates, including small molecules [28] and fluorescent proteins [29, 30] can be monitored for changes in cellular localization due to *S*-palmitoylation. Recently, we initiated a research program focused on developing new chemical tools that would allow us to probe the dynamic activity levels of the APTs in live cells. To accomplish this, we developed fluorescent probes that respond to *S*-deacylation of a peptide substrate with enhanced fluorescence (Fig. 1) [14, 24, 25]. The resultant family of depalmitoylation probes (DPPs; Fig. 2a–c) can monitor changes in APT activity levels by live cell fluorescence microscopy or flow cytometry. Although outside the scope of this chapter, we also recently developed ratiometric depalmitoylation probes (RDPs), which allow for better quantification of APT activity levels, including in complex primary tissue samples [31].

Among the first-generation DPPs, DPP-2, reports on general cytosolic activity (Fig. 2a, Fig. 3 and 4), while DPP-3 is more selective for APT1 over APT2 [24]. These probes use a surrogate C-8 lipid substrate to increase cell uptake. DPP-1 used a natural palmitate lipid, but due to solubility issues is only applicable to *in vitro* assays. DPP-5, however, features an additional water solubilizing group on the scaffold (Fig. 2b), which allows for the use of natural palmitate group and measurement of depalmitoylation (rather than peptide *S*-deacylation) [25]. Finally, mitoDPP-2 and mitoDPP-3 feature a triphenylphosphonium group (Fig. 2c), which shuttles the probes to the mitochondria and reports on APT activity selectively within this compartment [14]. Here, we will describe the general use of the DPP

family of probes to measure APT activities both *in vitro* and in live biological samples, using cytosolic and mitochondrial activity measurements as example experiments.

2. Materials

1. 384-well black flat bottom plate
2. Infinite M200 Pro plate reader (Tecan)
3. Poly-D-Lysine (30–70 KDa)
4. Sterile water
5. 8-well imaging dish
6. MitoTracker Deep Red FM
7. Hoechst 33342
8. Palmostatin B
9. Live Cell Imaging Solution
10. HEPES Buffer: 20 mM HEPES, 150 mM NaCl and 0.1% Triton X-100 at pH 7.4.
11. 5 mM DPP-1 in DMSO, stored at -80°C
12. 1 and 5 mM DPP-2 in DMSO, stored at -80°C
13. 1 mM DPP-5 in DMSO, stored at -80°C
14. 0.5 mM mitoDPP-2 in DMSO, stored at -80°C .
15. 100 μM MitoTracker Deep Red in DMSO, stored at -80°C .
16. 1 mM Hoechst 33342 in DMSO, stored at -80°C .
17. 1 $\mu\text{g}/\mu\text{L}$ Poly-D-Lysine in sterile H_2O , stored at -20°C .
18. HeLa cells from ATCC, freeze at an early passage (passage 6) in individual aliquots. Use cells for fewer than 25 passages for all experiments.
19. Growth medium: DMEM glutamax, 10% FBS, 1% Pencillin/Streptomycin antibiotic mixture

Fluorescence microscopy

1. Lieca DMI8 epifluorescence microscope with Leica LASX software.
2. Hamamatsu Orca-Flash 4.0 camera.
3. 63x oil objective (N/A 1.4).
4. Images were taken in four channels: brightfield, Hoechst 33342 (ET 402/15x, Quad-S, ET 455/50m), MitoTracker Deep Red (ET 645/30x, Quad-S, ET 705/72m) and DPPs/mitoDPPs (YFP filter cube 1525306).

3. Methods

Detailed synthetic procedures for the preparation of DPP-1, DPP-2, DPP-5 and mitoDPP-2 can be accessed from previous reports [14, 24, 25]. This chapter will focus on optimal utilization of these chemical tools to report activity of *S*-depalmitoylases in *in vitro* biochemical and live cell imaging experiments.

3.1 *In vitro* S-depalmitoylation assays with purified APTs

We present here a number of steps to study biochemical activity of APTs *in vitro* using DPPs. As a representative case, the following steps involve a fluorescence plate reader assay to monitor the *in vitro* reaction kinetics of recombinant APT1 with DPP-2. (*see* Notes 1–6)

1. Warm HEPES Buffer at 37 °C.
2. Add 50 μ L of 7.5 μ M DPP-2 in HEPES Buffer to a 384-well plate.
3. Place the 384-well plate in plate reader at 37 °C for 3–5 min.
4. Add 25 μ L of either HEPES Buffer alone or HEPES Buffer containing 150 nM recombinant APT1 (*see* Notes 1–3) using a multi-channel pipette. The final concentration of DPP-2 and APT1 are 5 μ M and 50 nM, respectively.
5. To obtain a kinetic curve, measure fluorescence intensities every 30 s until the fluorescence emission saturates. Use the following parameters to run a kinetic assay using the Infinite M200 Pro plate reader: λ_{ex} 490/9 nm, λ_{em} 545/20 nm, Gain 70, No. of flashes 25, Integration time 100 μ s and Z-position 20000 μ m. These parameters need to be optimized for other plate readers.
6. Take the average of fluorescence emission for three experimental replicates for every time interval.
7. Normalize the average fluorescence emission of both control \pm APT1 to the average emission for control at $t = 0$.
8. Plot kinetic curves from normalized emission (Fig. 3a) to reveal the enzymatic activity of APT1. To obtain kinetic parameters, vary the concentration of probe, generally from approximately 50 nM to 20 μ M and repeat this protocol to obtain initial rates (*see* Ref [25]).
9. To compare an end point fluorescence emission spectra between control \pm APT1, at the end of the kinetic run in step 5, obtain emission spectra. We use the following parameters to obtain emission spectra: λ_{ex} 485 nm, λ_{em} 510–700 nm, Gain 100, No. of flashes 25, Integration time 100 μ s and Z-position 20,000 μ m. Normalize average fluorescence intensities for three biological replicates at all wavelengths for both control \pm APT1 to maximum fluorescence intensity for control (\sim 543 nm).
10. Plot normalized emission to wavelength (Fig. 3b) to demonstrate APT1 activity.

3.2 Poly-D-Lysine coating of imaging dishes

Detachment of cells from the surface of imaging dish during a number of washing steps can be a problem depending on cell lines. As a precautionary measure, we use Poly-D-Lysine to coat our dishes to improve cell adherence to the imaging surface (*see Note 7*).

1. Perform all following steps in a biosafety cabinet to maintain sterility.
2. Add 50 μL of Poly-D-Lysine stock solution (1 $\mu\text{g}/\mu\text{L}$) to 5 mL of sterile water for a final concentration of 0.01 $\mu\text{g}/\mu\text{L}$.
3. Add 400 μL of 0.01 $\mu\text{g}/\mu\text{L}$ of Poly-D-Lysine to each well of the 8-well imaging dish at room temperature.
4. After 2 h, remove the solution from each well of the dish. The treated dish is now ready for plating cells.

3.3 Epifluorescence Imaging of DPP-2/DPP-5/mitoDPP-2 with PalmB

1. Plate HeLa cells (50000–55000/well) in 450 μL of growth media into an 8-well dish (*see Note 8*).
2. After 24–28 h, remove the growth media and wash the cells with 400 μL of DMEM glutamax.
3. Add 400 μL of DMEM glutamax containing 1 μM Hoechst 33342, 100 nM MitoTracker Deep Red and 5 μM PalmB/equivalent DMSO, or other experimental variable (*see Note 9 and 10*).
4. Incubate the cells at 37 °C with a supply of 5% CO_2 .
5. After 30 min of incubation, wash the cells with 400 μL of Live Cell Imaging Solution and replace by 1 μM DPP-2/1 μM DPP-5/500 nM mitoDPP-2 in 400 μL of Live Cell Imaging Solution (*see Note 11*). To minimize experimental variability due to pipetting error, we recommend making one master stock of DPP and then splitting it between the wells in an experiment (*see Note 12 and 13*).
6. After 15 min of incubation at 37 °C with a supply of 5% CO_2 , acquire images on an inverted epifluorescence microscope (*see Note 14–17*). We recommend using the MitoTracker Deep Red channel for focusing the objective lens on cells to minimize photobleaching of the DPP signal.

3.4 Details of quantification of images

Images are quantified using Fiji (Image J, Wayne Rasband, NIH), which is available free of cost. Fiji is a very versatile software and provides different ways to quantify and process images for publication purposes. We recommend using the Fiji online resources for in-depth training on the software. Nevertheless, in this section we will briefly discuss the simplest way to process images, which we have found provides consistent results.

1. Use *free hand selection* tool from Fiji tool bar to select region of interest in the brightfield image, which comprises healthy cells that are on the same plane.

Ideally, this step is researcher “blinded”, where the images from various experimental points are scrambled to avoid bias in the analysis.

2. Open the ROI manager window, which is available under ‘*Analyze*’ and then ‘*Tool*’ option on the menu bar.
3. Add the region of interest selected in step 1 into ROI manager window.
4. Gate the selected region of interest from step 1 in corresponding MitoTracker image by clicking first on MitoTracker image and then on the code for the region of interest in ROI window.
5. Press ‘*m*’ on the keyboard to get the mean fluorescence intensity from MitoTracker image.
6. Repeat steps 4 and 5 for the corresponding image for DPP-2/DPP-5/mitoDPP-2.
7. Use mean fluorescence intensities for all the images to calculate average fluorescence intensity and standard errors for both MitoTracker channel and DPP-2/DPP-5/mitoDPP-2 channel.
8. Normalize average fluorescence intensity for both MitoTracker and DPPs/ mitoDPPs for various set of conditions to the control experiment to show relative effect of external perturbations on mitochondrial health and APTs activity, respectively.

4. Notes

1. For purification of recombinant APT1 and APT2 *see* Ref [24].
2. The purified APT1 and APT2 (not included here) should be aliquoted and stored at -80°C . Avoid repeated freeze-thaws; it is preferable to use the purified enzyme once after thawing.
3. Additionally, we found that the activity of both APT1 and APT2 decrease with time, even when stored at -80°C . Thus, for optimal results, purify APT1 and APT2 right before use.
4. The core fluorophore constructs of DPP-5 and mitoDPP-2 are slightly different from that of the first generation depalmitoylation probe, DPP-2 (Fig. 2). APT activity on DPP-5 and mitoDPP-2 release fluorescent products that are brighter than the product from DPP-2. Therefore *in vitro* assays can be run on lower concentrations of probes. *See* Refs [14, 25].
5. The *in vitro* depalmitoylation assay presented here can be extended to assays with cell lysates or Immunoprecipitated proteins.
6. To demonstrate enzymatic depalmitoylation by cell lysates or immunoprecipitated proteins, PalmB is recommended as a control for *in vitro* APT activity, as in our hands PalmB is a robust pan-active APT inhibitor that can be used to distinguish between enzymatic and non-enzymatic *S*-depalmitoylation activities. We recommend using $5\ \mu\text{M}$ to $20\ \mu\text{M}$ PalmB in incubations with cell

lysates or immunoprecipitated proteins for 20 min before addition of DPPs/ mitoDPPs.

7. For some cells, Poly-D-lysine may be toxic, in which case lower concentrations or other adherents can be used.
8. Depending on growth conditions and cell health, the cell number and resultant density of cells for imaging may need to be optimized.
9. Treatment with PalmB and APT1/APT2 specific inhibitors ML348/ML349 [26] (not included in this work), respectively, should always be done in plain DMEM glutamax, as we have seen that activity of these inhibitors is reduced by the presence of fetal bovine serum.
10. For experiments just requiring MitoTracker and Hoechst staining (*e.g.*, shRNA/ siRNA silencing, genetic overexpression *etc.*), growth medium can be used for incubation of cells with these cell markers.
11. To avoid detachment of cells from the imaging surface during the imaging experiments all the washing and addition of various probes should be done very gently. The addition of solutions should preferably be done along the sides of imaging dishes.
12. There are many steps which can contribute to technical variability in an experiment *e.g.*, pipetting errors, different stocks of probes, non-uniform intensity of light source (especially at the end of its life span). Therefore, to minimize false results from these technical issues we recommend running experiments with the control conditions in parallel.
13. Since the kinetics of DPPs and mitoDPPs are very fast, for experiments where one might expect only subtle changes in activity of APTs due to external stimulation (*e.g.*, EGF treatment, starvation, palmitate stress, *etc.*), multichannel pipettes are recommended to add probes solution simultaneously in both control and treatment conditions.
14. We generally do imaging after 15 min of incubation (which includes 10–12 min of incubation at 37 °C and roughly 3–5 min to get the dishes ready on microscope for imaging) with probes. Nevertheless, one can try to obtain images from earlier time points if the experiment demands. We have found that the experimental error from earlier time points is generally higher.
15. We recommend imaging experiments in sets (treatment vs. control) to obtain the highest quality data, which minimizes image acquisition time, resulting in lower experimental error. Alternatively, image acquisition on a microscope capable of autofocussing and processing many samples in a short time is recommended.
16. For acquiring images, we recommend taking one or two images per well from all of the samples. Then, collect a second set of images from all of the samples, ultimately collecting three to five images from each well. Collecting images in this way helps to decrease bias due to timing.

17. In our experience, it takes 7–10 min to acquire 5–6 high quality images for a set of samples. Therefore, for fairly representing images, we recommend users deploy the entire set of images for quantification purposes, but when selecting images to display, use images that were acquired at nearly the same time.

Acknowledgement

This work was supported by the University of Chicago, the National Institute of General Medical Sciences (R35 GM119840) of the National Institutes of Health, and a Research Fellowship from the Alfred P. Sloan Foundation.

References

1. Blanc M, David F, Abrami L et al. (2015) SwissPalm: Protein Palmitoylation database. *F1000Res* 4:261. [PubMed: 26339475]
2. Linder ME, Deschenes RJ (2007) Palmitoylation: policing protein stability and traffic. *Nat Rev Mol Cell Biol* 8:74–84. [PubMed: 17183362]
3. Lanyon-Hogg T, Faronato M, Serwa RA, Tate EW (2017) Dynamic Protein Acylation: New Substrates, Mechanisms, and Drug Targets. *Trends Biochem Sci* 42:566–581. [PubMed: 28602500]
4. Sanders SS, Martin DD, Butland SL et al. (2015) Curation of the Mammalian Palmitoylome Indicates a Pivotal Role for Palmitoylation in Diseases and Disorders of the Nervous System and Cancers. *PLoS Comput Biol* doi: 10.1371/journal.pcbi.1004405
5. Hernandez JL, Majmudar JD, Martin BR (2013) Profiling and inhibiting reversible palmitoylation. *Curr Opin Chem Biol* 17:20–26. [PubMed: 23287289]
6. Peng T, Thion E, Hang HC (2016) Proteomic analysis of fatty-acylated proteins. *Curr Opin Chem Biol* 30:77–86. [PubMed: 26656971]
7. Gottlieb CD, Linder ME (2017) Structure and function of DHHC protein S-acyltransferases. *Biochem Soc Trans* 45:923–928. [PubMed: 28630137]
8. Rana MS, Kumar P, Lee CJ et al. (2018) Fatty acyl recognition and transfer by an integral membrane S-acyltransferase. *Science* 359.
9. Zhong B, DeRan M, Li X, et al. (2013) 2-Bromopalmitate analogues as activity-based probes to explore palmitoyl acyltransferases. *J Am Chem Soc* 135:7082–7085. [PubMed: 23631516]
10. Duncan JA, Gilman AG (2002) Characterization of *Saccharomyces cerevisiae* acyl-protein thioesterase I, the enzyme responsible for G protein alpha subunit deacylation in vivo. *J Biol Chem* 277:31740–31752. [PubMed: 12080046]
11. Lin DT, Conibear E (2015) ABHD17 proteins are novel protein depalmitoylases that regulate N-Ras palmitate turnover and subcellular localization. *Elife* 4:e11306. [PubMed: 26701913]
12. Toyoda T, Sugimoto H, Yamashita S (1999) Sequence, expression in *Escherichia coli*, and characterization of lysophospholipase II. *Biochim Biophys Acta* 1437:182–193. [PubMed: 10064901]
13. Verkruyse LA, S. Hofmann SL (1996) Lysosomal targeting of palmitoyl-protein thioesterase. *J Biol Chem* 271:15831–15836. [PubMed: 8663305]
14. Kathayat RS, Cao Y, Elvira PD et al. (2018) Active and dynamic mitochondrial S-depalmitoylation revealed by targeted fluorescent probes. *Nat Commun* 9:334. [PubMed: 29362370]
15. El-Husseini Ael D, Schnell E, Dakoji S et al. (2002) Synaptic strength regulated by palmitate cycling on PSD-95. *Cell* 108:849–863. [PubMed: 11955437]
16. Ponimaskin E, Dityateva G, Ruonala MO, et al. (2008) Fibroblast growth factor-regulated palmitoylation of the neural cell adhesion molecule determines neuronal morphogenesis. *J Neurosci* 28:8897–8907. [PubMed: 18768683]
17. Drisdell RC, Green WN (2004) Labeling and quantifying sites of protein palmitoylation. *Biotechniques* 36:276–285. [PubMed: 14989092]
18. Wan J, Roth AF, Bailey AO, Davis NG (2007) Palmitoylated proteins: purification and identification. *Nat Protoc* 2:1573–1584. [PubMed: 17585299]

19. Forrester MT, Hess DT, Thompson JW et al. (2011) Site-specific analysis of protein Sacylation by resin-assisted capture. *J Lipid Res* 52:393–398. [PubMed: 21044946]
20. Percher A, Ramakrishnan S, Thinon E et al. (2016) Mass-tag labeling reveals sitespecific and endogenous levels of protein S-fatty acylation. *Proc Natl Acad Sci U S A* 113:43024307.
21. Charron G, Wilson J, Hang HC (2009) Chemical tools for understanding protein lipidation in eukaryotes. *Curr Opin Chem Biol* 13:382–391. [PubMed: 19699139]
22. Martin BR, Wang C, Adibekian A, Tully SE, Cravatt BF (2011) Global profiling of dynamic protein palmitoylation. *Nat Methods* 9:84–89. [PubMed: 22056678]
23. Yap MC, Kostiuk MA, Martin DD et al. (2010) Rapid and selective detection of fatty acylated proteins using omega-alkynyl-fatty acids and click chemistry. *J Lipid Res* 51:15661580.
24. Kathayat RS, Elvira PD, Dickinson BC (2017) A fluorescent probe for cysteine depalmitoylation reveals dynamic APT signaling. *Nat Chem Biol* 13:150–152. [PubMed: 27992880]
25. Qiu T, Kathayat RS, Cao Y, Beck MW, Dickinson BC (2018) A Fluorescent Probe with Improved Water Solubility Permits the Analysis of Protein S-Depalmitoylation Activity in Live Cells. *Biochemistry* 57:221–225. [PubMed: 29023093]
26. Adibekian A, Martin BR, Chang JW et al. (2012) Confirming Target Engagement for Reversible Inhibitors in Vivo by Kinetically Tuned Activity-Based Probes. *Journal of the American Chemical Society* 134:10345–10348. [PubMed: 22690931]
27. Garland M, Schulze CJ, Foe IT et al. (2018) Development of an activity-based probe for acyl-protein thioesterases. *PLoS One* 13:e0190255. [PubMed: 29364904]
28. Creaser SP, Peterson BR (2002) Sensitive and rapid analysis of protein palmitoylation with a synthetic cell-permeable mimic of SRC oncoproteins. *J Am Chem Soc* 124:2444–2445. [PubMed: 11890786]
29. Dekker FJ, Rocks O, Vartak N (2010) Small-molecule inhibition of APT1 affects Ras localization and signaling. *Nature Chemical Biology* 6:449. [PubMed: 20418879]
30. Görmer K, Bürger M, Kruijtzter JA et al. (2012) Chemical-biological exploration of the limits of the Ras de- and repalmitoylating machinery. *Chembiochem* 13:1017–1023. [PubMed: 22488913]
31. Beck M, Kathayat RS, Cham CM, Chang EB, Dickinson BC (2017) Michael additionbased probes for ratiometric fluorescence imaging of protein S-depalmitoylases in live cells and tissues. *Chemical Science* 8:7588–7592. [PubMed: 29568422]

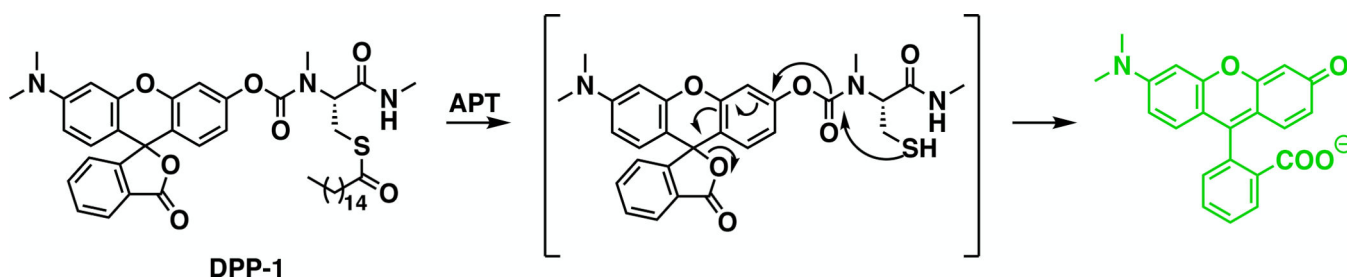


Figure 1.

Schematic of mechanism of DPPs, which “*turn-on*” when processed by acyl protein thioesterases (APTs). A peptide substrate featuring an acylated cysteine residue is tethered to a pro-fluorescent molecule by a biologically stable carbamate linker. APT s activity on the peptide and removal of the thioester unmasks the thiol of the cysteine, which results in a cascade of rapid intramolecular cyclization, lactone opening, and release of a fluorescent product.

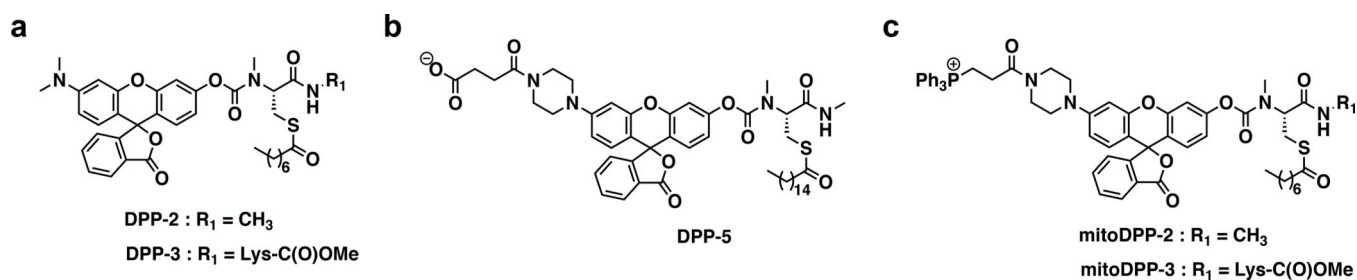


Figure 2. Structures of a subset of the delpamitoylation probes (DPPs) for APT activity. **(a)** First-generation untargeted *S*-deacylase probe DPP-2 and more APT1-targeted deacylase probe DPP-3. **(b)** Second-generation *S*-depalmitoylase probe with enhanced water solubility, DPP-5. **(c)** Mitochondrial-targeted derivatives of DPP-2 and DPP-3, mitoDPP-2 and mitoDPP-3.

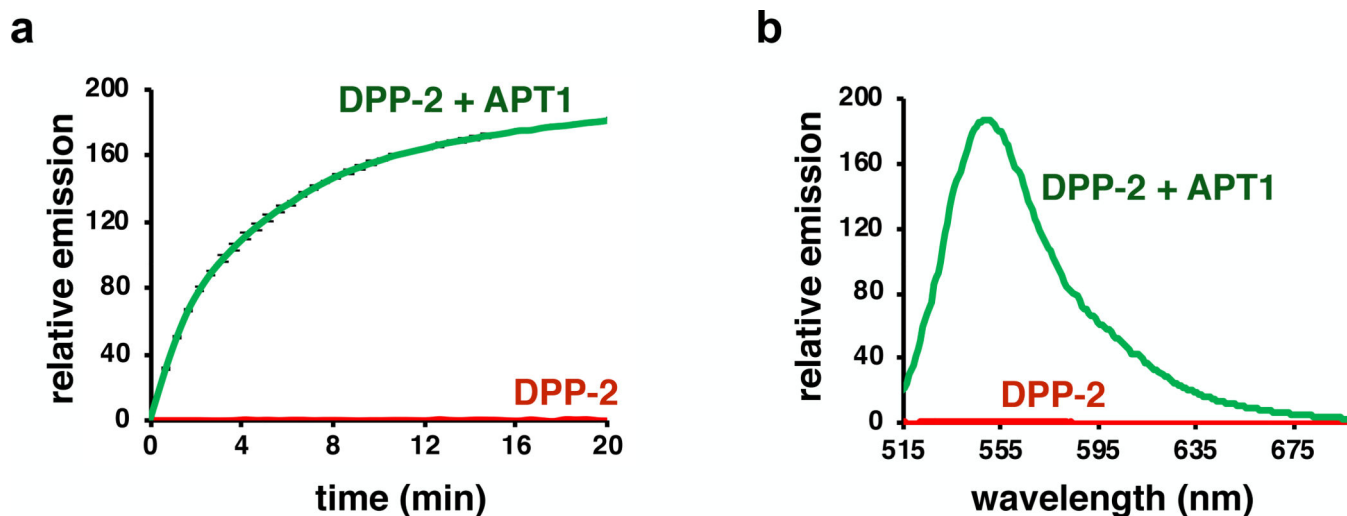


Figure 3.

A representative *in vitro* biochemical assay of DPP-2 with recombinant APT1. (a) Normalized *in vitro* fluorescence assays of 5 μ M DPP-2, incubated with or without 50 nM purified APT1 (λ_{ex} 490/9 nm, λ_{em} 545/20 nm) in HEPES Buffer (20 mM, pH 7.4, 150 mM NaCl, 0.1% Triton X-100). Error bars are standard error (n = 3). (b) Normalized fluorescence emission spectrum of 5 μ M DPP-2, incubated with or without 50 nM APT1 for 20 min (λ_{ex} = 485 nm). Spectra are plotted as average of n = 3.

